Wasserstein Random Forests
and Applications in Heterogeneous Treatment Effects

Q. Du   G. Biau
Sorbonne Université, CNRS, LPSM
Paris, France

F. Petit   R. Porcher
Université de Paris, CRESS, INSERM, INRAE
Paris, France

Abstract

We present new insights into causal inference in the context of Heterogeneous Treatment Effects by proposing natural variants of Random Forests to estimate the key conditional distributions. To achieve this, we recast Breiman's original splitting criterion in terms of Wasserstein distances between empirical measures. This reformulation indicates that Random Forests are well adapted to estimate conditional distributions and provides a natural extension of the algorithm to multi-variate outputs. Following the philosophy of Breiman's construction, we propose some variants of the splitting rule that are well-suited to the conditional distribution estimation problem. Some preliminary theoretical connections are established along with various numerical experiments, which show how our approach may help to conduct more transparent causal inference in complex situations. A `Python` package is also provided.

1   Introduction

One of the primary objectives of supervised learning is to provide an estimation of the conditional expectation $\mathbb{E}\left[Y \mid X = x\right]$ for some underlying 1-dimensional objective Y and a multidimensional covariate X given the dataset $\mathcal{D}_n = \{(X_i, Y_i) : 1 \leq i \leq n\}$. However, in many real-world applications, it is also important to extract the additional information encoded in the conditional distribution $\mathcal{L}\left(Y \mid X = x\right)$. This is particularly the case in the field of Heterogeneous Treatment Effects (HTE) estimation problems, which represent the main motivation of this work.

1.1   Motivation

In HTE problems, the traditional object of interest is the Conditional Average Treatment Effect (CATE) function, defined by

$$\tau(x) = \mathbb{E}\left[Y(1) - Y(0) \mid X = x\right], \tag{1}$$

where $Y(1)$ (resp. $Y(0)$) denotes the potential outcome (e.g., Rubin, 1974; Imbens and Rubin, 2015) of the treatment (resp. no treatment). The propensity score function $e(\cdot)$ is defined by

$$e(x) = \mathbb{P}\left(T = 1 \mid X = x\right),$$

which captures the probability of receiving the treatment for each individual. The data are usually of the form $\bar{\mathcal{D}}_n = \{(X_i, Y_i(T_i), T_i) : 1 \leq i \leq n\}$, where T_i denotes the treatment assignment indicator. Recently, many approaches based on modern statistical learning techniques have been investigated to estimate the CATE function (e.g., Künzel et al., 2019; Athey and Wager, 2019; Nie and Wager, 2017). Typically, assuming unconfoundedness, that is

$$(Y(0), Y(1)) \perp\!\!\!\perp T \mid X , \tag{2}$$

and that the propensity score function is uniformly bounded away from 0 and 1, one is able to estimate $\mu_0(x) = \mathbb{E}\left[Y(0) \mid X = x\right]$ and $\mu_1(x) = \mathbb{E}\left[Y(1) \mid X = x\right]$, respectively with

$$\{(X_i, Y(T_i)) : T_i = 0\} \text{ and } \{(X_i, Y(T_i)) : T_i = 1\}. \tag{3}$$

The classical approach in the HTE context is to design the causal inference procedure around the estimation of the CATE function $\tau(\cdot)$ defined in (1) using $\bar{\mathcal{D}}_n$, and to test whether there is a notable difference between $\tau(x)$ and 0 for each new coming individual x. It is important to note that this is already a difficult task for certain datasets due to the unbalance between treatment and control groups or other practical reasons. For instance, the X-learner (Künzel et al., 2019) is proposed to deal with the unbalanced design by making efficient use of the structural information about the CATE function, and the R-learner

(Nie and Wager, 2017) is introduced to improve accuracy and robustness of the CATE function estimation by formulating it into a standard loss-minimization problem. However, a simple inference based on the CATE function, or other key features composed by the average treatment effects. (e.g., the sorted Group Average Treatment Effects (GATES) proposed by Chernozhukov et al. 2018), may be hazardous in some situations because of the lack of information on the fluctuations, or multimodality, of both conditional laws $\mathcal{L}(Y(0) \mid X = x)$ and $\mathcal{L}(Y(1) \mid X = x)$. This phenomenon, in practice, can arise when $Y(0)$ and/or $Y(1)$ depend on some additional unconfounding factors that are not collected in the study, which, however, greatly affect the behaviors of the potential outcomes. From another point of view, being aware of the existence of such problems may also help to fix the flaw of data collection procedure or the lack of subgroup analysis for future study.

Ideally, one is interested in estimating the joint conditional distribution $\mathcal{L}((Y(0), Y(1)) \mid X = x)$. Unfortunately, a major difficulty of HTE estimation lies in the fact that it is in general impossible to collect $Y_i(0)$ and $Y_i(1)$ at the same time for the point X_i. Unlike the difference in the linear conditional expectation $\tau(\cdot)$, the dependence between $Y(0)$ and $Y(1)$ given X is much more complex and difficult to track. Hence, due to the lack of information of the collectable dataset, the estimation of the conditional covariance between $Y(0)$ and $Y(1)$ is usually unavailable, let alone the conditional joint distribution. A possible route to address this shortcoming is to concentrate on a weaker problem: instead of estimating $\mathcal{L}((Y(0), Y(1)) \mid X = x)$, we are interested in the estimation of conditional marginal distributions $\mathcal{L}(Y(0) \mid X = x)$ and $\mathcal{L}(Y(1) \mid X = x)$. By considering the two subgroups (3) of the dataset $\bar{\mathcal{D}}_n$, the problem thus enters into a more classical supervised learning context, similar as the design of T-learners (Künzel et al., 2019), while the objective is replaced by the estimation of conditional distributions. In some scenarios, even a simple raw visualization of the marginal conditional distributions, as a complement of CATE function estimation, may greatly help the decision making process for practitioners.

Another motivation comes from the need to set-up statistically sound decision procedures for multivariate objectives in the context of HTE. For example, a treatment is often related to a cost, which is also collectable and sometimes essential to the final treatment decisions. In this context, a simple extension of the CATE function will clearly not be able to capture the dependencies between the treatment effects and the cost. Thus, a statistical tool that allows conditional distribution estimation with multivariate ob-

jective will therefore be useful for more complex inferences involving both treatment effects and costs at the same time. In general, the traditional nonparametric methods for conditional distribution inference (e.g., Hall et al., 1999; Hall and Yao, 2005) are less effective when it comes to flexibility of implementation, parallelization, and the ability to handle high-dimensional noisy data. Another remark is that Gaussian Process-based methods (e.g., Dutordoir et al., 2018) usually require the existence of density w.r.t. Lebesgue measure, which is not always true in the context of HTE. So, our goal is to achieve density-free conditional distribution estimation based on available modern machine/statistical learning tools.

1.2 Random Forests for conditional distribution estimation

In order to address the issues described in the subsection above, our idea is to propose an adaptation of the Random Forests (RF) algorithm (Breiman, 2001), so that it can be applied to the conditional distribution estimation problems in the HTE context. RF have proven to be successful in many real-world applications—the reader is referred to Biau and Scornet (2015) and the references therein for a general introduction. If we look at the final prediction at each point x provided by the RF algorithm, it can be regarded as a weighted average of $(Y_i : 1 \le i \le n)$, where the random weights depend upon the training dataset and the stochastic mechanism of the forests. Therefore, a very natural idea is to use this weighted empirical measure to approximate the target conditional distribution. This is also the driving force in the construction of Quantile Regression Forests (Meinshausen, 2006; Athey et al., 2019) and other approaches that combine kernel density estimations and Random Forests (e.g., Pospisil and Lee, 2019; Hothorn and Zeileis, 2017).

In the present article, instead of studying the quantile or density function of the target conditional distribution, we focus directly on the (weighted) empirical measures output by the forests and the associated Wasserstein distances. This also makes further inferences based on Monte-Carlo methods or smoothing more convenient and straightforward. To make it clearer, let us denote by $\pi(x, dy)$ the probability measure associated with the conditional distribution $\mathcal{L}(Y \mid X = x)$. Heuristically speaking, if the Wasserstein distance between the Markov kernels $\pi(x, dy)$ and $\pi(z, dy)$ is dominated, in some sense, by the distance between x and z, then the data points that fall into a "neighborhood" of x are expected to be capable of providing reliable approximation of the conditional measure $\pi(x, dy)$. In the RF context, the role of each tree in the ensemble

is to build a wisely created partition of the domain, so that the "neighborhood" mentioned above can be defined accordingly. As such, the random weights come from the averaging procedure of multiple trees.

As Breiman's original RF are primarily designed for conditional expectation estimations, we first provide in Section 2 a reformulation that gives new insights into Breiman's original splitting criterion, by exploiting a simple relation between empirical variance and Wasserstein distance between empirical measures. This reformulation allows a new interpretation of the RF algorithm in the context of conditional distribution estimation, which, in turn, can be used to handle multivariate objectives with a computational cost that grows linearly with the dimension of the output. We also investigate in this section several dedicated modifications of Breiman's splitting rule and present some preliminary theoretical connections between their constructions. With a slight abuse of language, all these RF variants aiming at conditional distribution estimation are referred to as Wasserstein Random Forests (WRF) in this article. Finally, we return in Section 3 to the HTE problem and illustrate through various numerical experiments how WRF may help to design more transparent causal inferences in this context.

2 Wasserstein Random Forests

In order to simplify the introduction of WRF, we temporarily limit the discussion to the classical supervised learning setting. Let $X \in \mathbb{R}^d$ and $Y \in \mathbb{R}^{d'}$ be, respectively, the canonical random variables of covariate and the objective. Our goal is to estimate the conditional measure $\pi(x, dy)$ associated with $\mathcal{L}(Y \mid X = x)$ using the dataset $\mathcal{D}_n = \{(X_i, Y_i) : 1 \leq i \leq n\}$.

2.1 Mechanism of Random Forests

A Random Forest is an ensemble method that aggregates a collection of randomized decision trees. Denote by M the number of trees and, for $1 \leq j \leq M$, let Θ_j be the canonical random variable that captures randomness of the j-th tree. Each decision tree is trained on a randomly selected dataset $\mathcal{D}_n^*(\Theta_j)$ with the same cardinal $a_n \in \{2, \ldots, n\}$, sampled uniformly in $\mathcal{D}_n$ with or without replacement. More concretely, for each tree, a sequence of axis-aligned splits is made recursively by maximizing some fixed splitting rule. At each iteration, **mtry** $\in \{1, \ldots, d\}$ directions are explored and the splits are always performed in the middle of two consecutive data points, in order to remove the possible ties. The splitting stops when the current cell contains fewer points than a threshold **nodesize** $\in \{2, \ldots, a_n\}$, or when all the data points are identical. In this way, a binary hierarchical parti-

tion of $\mathbb{R}^d$ is constructed. For any $x \in \mathbb{R}^d$, we denote by $A_n(x; \Theta_j, \mathcal{D}_n)$ the cell in the j-th tree that contains x and by $N_n(x; \Theta_j, \mathcal{D}_n)$ the number of data points in $\mathcal{D}_n^*(\Theta_j)$ that fall into $A_n(x; \Theta_j, \mathcal{D}_n)$.

The core of our approach relies on the fact that the prediction $\pi_n(x, dy; \Theta_j, \mathcal{D}_n)$ of the conditional distribution at point x given by the j-th tree is simply the empirical measure associated with the observations that fall into the same cell $A_n(x; \Theta_j, \mathcal{D}_n)$ as x, that is

$$\pi_n(x, dy; \Theta_j, \mathcal{D}_n) = \sum_{i \in \mathcal{D}_n^*(\Theta_j)} \frac{\mathbf{1}_{\{X_i \in A_n(x; \Theta_j, \mathcal{D}_n)\}}}{N_n(x; \Theta_j, \mathcal{D}_n)} \delta_{Y_i}(dy),$$

where $\delta_{Y_i}(dy)$ is the Dirac measure at Y_i. Let $\Theta_{[M]} = (\Theta_1, \ldots, \Theta_M)$. As such, the final estimation $\pi_{M,n}(x, dy; \Theta_{[M]}, \mathcal{D}_n)$ provided by the forest is but the average of the $\pi_n(x, dy; \Theta_j, \mathcal{D}_n)$, $1 \leq j \leq M$, over the M trees, i.e.,

$$\pi_{M,n}(x, dy; \Theta_{[M]}, \mathcal{D}_n) = \frac{1}{M} \sum_{j=1}^{M} \pi_n(x, dy; \Theta_j, \mathcal{D}_n).$$

Equally, $\pi_{M,n}(x, dy; \Theta_{[M]}, \mathcal{D}_n) = \sum_{i=1}^{n} \alpha_i(x) \delta_{Y_i}(dy)$, where $\alpha_i(x) = \sum_{j=1}^{M} \frac{\mathbf{1}_{\{X_i \in A_n(x; \Theta_j, \mathcal{D}_n)\}}}{M N_n(x; \Theta_j, \mathcal{D}_n)} \mathbf{1}_{\{i \in \mathcal{D}_n^*(\Theta_j)\}}$ is the random weight associated with Y_i. It is readily checked that $\sum_{i=1}^{n} \alpha_i(x) = 1$ for any $x \in \mathbb{R}^d$. Thus, the final prediction $\pi_{M,n}(x, dy; \Theta_{[M]}, \mathcal{D}_n)$ is a weighted empirical measure with random weights naturally given by the tree aggregation mechanism. Our notation is compatible with Biau and Scornet (2015), where a more detailed introduction to RF is provided. It should be stressed again that we are interested in learning the conditional distribution $\mathcal{L}(Y \mid X = x)$, not in inferring the conditional expectation $\mathbb{E}[Y \mid X = x]$ as in traditional forests. This is of course a more complex task, insofar as the expectation is just a feature, albeit essential, of the distribution.
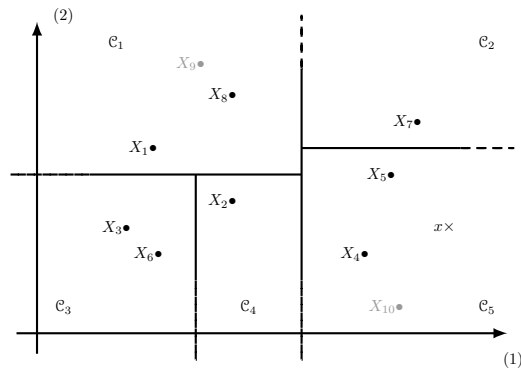
Figure 1: Illustration of the a single decision tree. Note that X_9 and X_{10} are not sampled in the sub-dataset used for the tree's construction.

As an illustration, consider in Figure 1 the partition $\mathcal{C}_1 \cup \mathcal{C}_2 \cup \mathcal{C}_3 \cup \mathcal{C}_4 \cup \mathcal{C}_5 = \mathbb{R}^2$ provided by a decision tree

trained on a bidimensional sub-dataset of size 8. The estimation of the conditional distribution at the point x is simply the empirical measure $\frac{1}{2}(\delta_{Y_4} + \delta_{Y_5})$ associated with the cell $\mathcal{C}_5$ to which it belongs. Mutatis mutandis, suppose that there is another decision tree that gives the measure $\frac{1}{2}(\delta_{Y_5} + \delta_{Y_7})$ as the estimation at x. Then the final estimation of the conditional distribution output by the forest that contains these two trees is the empirical distribution $\frac{1}{4}\delta_{Y_4} + \frac{1}{2}\delta_{Y_5} + \frac{1}{4}\delta_{Y_7}$. On the other hand, the classical RF outputs the average $\frac{1}{4}Y_4 + \frac{1}{2}Y_5 + \frac{1}{4}Y_7$ as the scalar estimation of the conditional expectation.

2.2 Breiman's Splitting criteria

Now, let us take a closer look at the splitting criteria that are maximized at each cell in the construction of trees. For a cell that consists in a subset of data points $A \subset \mathcal{D}_n$, an axis-aligned cut along the k-th coordinate at position z defines a partition $A_L \cup A_R$ of A. More precisely, we denote

$$A_L = \left\{ (X_i, Y_i) \in A : X_i^{(k)} \leq z \right\}$$

and

$$A_R = \left\{ (X_i, Y_i) \in A : X_i^{(k)} > z \right\}.$$

With a slight abuse of notation, we write $X_i \in A$ when $(X_i, Y_i) \in A$. Recall that Breiman's original splitting criterion (Breiman, 2001) takes the following form:

$$L_B(A_L, A_R) = \frac{1}{N_A} \sum_{X_i \in A} (Y_i - \bar{Y}_A)^2$$
$$- \frac{1}{N_A} \sum_{X_i \in A_L} (Y_i - \bar{Y}_{A_L})^2 - \frac{1}{N_A} \sum_{X_i \in A_R} (Y_i - \bar{Y}_{A_R})^2,$$
$$(4)$$

where $\bar{Y}_A$ (resp. $\bar{Y}_{A_L}$, $\bar{Y}_{A_R}$) is the average of the Y_i that fall into A (resp. A_L, A_R), and N_A (resp. N_L, N_R) is the cardinal of A (resp. A_L, A_R). This criterion is maximized at each node of each tree over z and the **mtry** randomly chosen coordinates (see, e.g., Biau and Scornet, 2015, section 2.2).

Remark 2.1. We recall that the Breiman's splitting criterion can be regarded as the gain induced by the cut in terms of empirical L^2-error. Hence, the mechanism of the construction of the decision tree can indeed be interpreted as a greedy optimization.

The quantity L_B can also be interpreted as the difference between the total variance and the intra-class variance within the subgroups divided by the split, which, thanks to the total variance decomposition, turns out to be the associated inter-class variance, i.e.,

$$L_B(A_L, A_R) = \frac{N_L}{N_A}(\bar{Y}_{A_L} - \bar{Y}_A)^2 + \frac{N_R}{N_A}(\bar{Y}_{A_R} - \bar{Y}_A)^2. \quad (5)$$

Remark 2.2. As mentioned in Remark 2.1, the representation (5) can be understood as the difference between the predictions with and without the cut, in terms of empirical L^2-error. In fact, for each data point at A_L (resp. A_R), the prediction with the split is $\bar{Y}_{A_L}$ (resp. $\bar{Y}_{A_R}$). At the same time, for all the data points in A, the predictions without the split are given by $\bar{Y}_A$. As such, the associated weights N_L/N_A (resp. N_R/N_A) come from the number of data points in the sub-cell A_L (resp. A_R). This reveals a different understanding of the Breiman's splitting rule as mentioned in Remark 2.1: When considering conditional expectation estimation, the split should be made such that the predictions given by the tree are as different as possible, in terms of empirical L^2-error.

Regardless of the choice of interpretation, since there is only a finite number of cuts to be evaluated at each iteration, a decision tree can therefore be built in a greedy manner. Without loss of generality, when bootstrap is involved (i.e., $\mathcal{D}_n^*(\Theta_j)$ is sampled with replacement), one may consider multisets/bags in order to deal with duplicate data for formal definitions discussed above. The details can be found in Algorithm 2.

2.3 Basic properties of Wasserstein distances

Before proceeding further, we recall some basic properties of Wasserstein distances. If not mentioned otherwise, d and d' denote respectively the dimension of the covariate X and the dimension of the objective Y. For $p \geq 1$, the Wasserstein distance $\mathcal{W}_p$ between two probability measures μ, ν on $\mathbb{R}^{d'}$ is defined by

$$\mathcal{W}_p(\mu, \nu) = \left(\inf_{\gamma \in \Gamma(\mu,\nu)} \int \|x - y\|^p \gamma(dx, dy) \right)^{\frac{1}{p}}, \quad (6)$$

where $\|\cdot\|$ is the Euclidean norm on $\mathbb{R}^{d'}$ and $\Gamma(\mu, \nu)$ denotes the set of all couplings of μ and ν, namely, $\gamma(dx, \mathbb{R}^{d'}) = \mu(dx)$ and $\gamma(\mathbb{R}^{d'}, dy) = \nu(dy)$. To guarantee that (6) is well-defined, it is necessary to assume that the p-th moments of both μ and ν are finite. When μ and ν are the probability measures on $\mathbb{R}$ (i.e., $d' = 1$), one can deduce that (see, e.g., Santambrogio, 2015)

$$\mathcal{W}_p(\mu, \nu) = \left(\int_0^1 \left| F_\mu^{-1}(u) - F_\nu^{-1}(u) \right|^p du \right)^{\frac{1}{p}}, \quad (7)$$

where $F_\mu^{-1}(u)$ (resp. $F_\nu^{-1}(u)$) is the generalized inverse distribution function defined by

$$F_\mu^{-1}(u) = \inf \left\{ x \in \mathbb{R} \mid F_\mu(x) \geq u \right\},$$

with $F_\mu(x)$ (resp. $F_\nu(x)$) the cumulative distribution function of μ (resp. ν). Thanks to (7), the Wasserstein

distance between empirical measures can be efficiently computed in the univariate case.

2.4 Intra-class interpretation

We focus on the representation of L_B given in (4). Denote by $\mu_N = \frac{1}{N} \sum_{i=1}^N \delta_{U_i}$. Observe that

$$\mathcal{W}_p^p(\mu_N, \delta_{V_1}) = \frac{1}{N} \sum_{i=1}^N \|U_i - V_1\|^p,$$

one can rewrite the Breiman's rule in terms of quadradic Wasserstein distances between empirical measures, namely,

$$L_B(A_L, A_R) = \frac{1}{2N_A} \sum_{X_i \in A} \mathcal{W}_2^2(\delta_{Y_i}, \pi_A)$$
$$- \frac{1}{2N_A} \sum_{X_i \in A_L} \mathcal{W}_2^2(\delta_{Y_i}, \pi_L) - \frac{1}{2N_A} \sum_{X_i \in A_R} \mathcal{W}_2^2(\delta_{Y_i}, \pi_R).$$
$$(8)$$

In the same spirit of Remark 2.1, the interpretation (8) heuristically indicates that RF are well-adapted to estimate conditional distributions. More precisely, the Breiman's rule can also be regarded as the gain in terms of quadratic Wasserstein error, induced by the split.

An important consequence of this result is that it allows a natural generalization of Breiman's criterion to outputs Y with a dimension greater than 1. Indeed, the extension of RF to multivariate outputs is not straightforward, even in the context of conditional expectation estimation (e.g., Segal and Xiao, 2011; Miller et al., 2014). The dependence between the different coordinates of the objective is usually dealt with using additional tuning or supplementary prior knowledge. Such a modeling is not necessary in our approach since dependencies in the Y-vector features are captured by the Wasserstein distances. (Note however that some appropriate normalization should be considered when there are noticeable differences between the coordinates of the objective.) Besides, this extension is also computationally efficient, as the complexity of the evaluation at each cell increases linearly w.r.t. the dimension d' of the objective Y. The details are provided in Algorithm 1. In the sequel, to increase the clarity of our presentation, we use the notation L_{intra}^2 instead of L_B for the criterion defined in (8).

2.5 Inter-class interpretation

Using the similar idea as mentioned in Remark 2.2 by replacing the L^2-error with the $\mathcal{W}_2$-distance between empirical measures according to the goal of conditional distribution estimation, it is natural to consider the

---

Algorithm 1: Computation of $L_{\text{intra}}^2(A_L, A_R)$ in the case $Y = (Y^{(1)}, Y^{(2)}, \ldots, Y^{(d')}) \in \mathbb{R}^{d'}$.

Require: Sub-datasets A_L, A_R and A.
Result: The value of $L_{\text{intra}}^2(A_L, A_R)$.

1 **for** $k \in \{1, 2, \ldots, d'\}$ **do**
2   Compute respectively
     $\bar{Y}_L^{(k)} = \frac{1}{N_L} \sum_{X_i \in A_L} Y_i^{(k)}$,
     $\bar{Y}_R^{(k)} = \frac{1}{N_R} \sum_{X_i \in A_R} Y_i^{(k)}$ and
     $\bar{Y}_A^{(k)} = \frac{1}{N_A} \sum_{X_i \in A} Y_i^{(k)}$.
3   Set respectively
     $W_L^{(k)} = \frac{1}{N_A} \sum_{X_i \in A_L} (Y_i^{(k)} - \bar{Y}_L^{(k)})^2$,
     $W_R^{(k)} = \frac{1}{N_A} \sum_{X_i \in A_R} (Y_i^{(k)} - \bar{Y}_R^{(k)})^2$ and
     $W_A^{(k)} = \frac{1}{N_A} \sum_{X_i \in A} (Y_i^{(k)} - \bar{Y}_A^{(k)})^2$.
4 **end**
5 Compute and output
   $\sum_{k=1}^{d'} \left(W_A^{(k)} - W_L^{(k)} - W_R^{(k)} \right)$.

---

following splitting criterion:

$$L_{\text{inter}}^p(A_L, A_R) = \frac{N_L}{N_A} \mathcal{W}_p^p(\pi_L, \pi_A) + \frac{N_R}{N_A} \mathcal{W}_p^p(\pi_R, \pi_A).$$

Remark 2.3. A very noticeable difference between intra-class and inter-class interpretation is that one does not need to choose a reference conditional distribution in the latter case. More precisely, at each data point (X_i, Y_i), we have used the reference conditional distribution δ_{Y_i} to build the associated local optimizer in terms of quadratic Wasserstein distance in (8). Such choice may not be informative enough in the case where the conditional distribution is, say, multimodal. However, in the inter-class interpretation, there is no such problem.

In the univariate case (i.e., $d' = 1$), thanks to (7), it is easily checked that L_{inter}^p can be computed with $\mathcal{O}(N_A \log(N_A))$ complexity at each cell that contains the data points $A \subset \mathcal{D}_n$. This rate can be achieved by considering a Quicksort algorithm in order to deal with the generalized inverse distribution function encountered in (7). The implementation is tractable, although slightly worse than $\mathcal{O}(N_A)$, the complexity of L_{intra}^2. However, the computation of the Wasserstein distance is not trivial when $d' > 1$, where an exact computation is of order $\mathcal{O}(N_A^3)$ (e.g., Peyré and Cuturi, 2018, Section 2). A possible relaxation is to consider an entropic regularized approximation such as Sinkhorn distance (e.g., Cuturi, 2013; Genevay et al., 2019; Lin et al., 2019), where the associated complexity is of order $\mathcal{O}(N_A^2/\epsilon^2)$ with tolerance $\epsilon \in (0, 1)$. Nevertheless, since the amount of evaluations of L_{inter}^p is enormous during the construction of RF, we only recommend using this variant of splitting criterion for

univariate problems at the moment. The details of efficient implementations and possible relaxations for multivariate cases will be left for future research. It is however now time to put our splitting analysis to good use and return to the HTE conditional distribution estimation problem.

3   Applications

Our primary interest is the improvement that WRF can bring into the causal inference under the potential outcomes framework. As for now, the potential outcomes $Y(0)$ and $Y(1)$ are assumed to be univariate random variables—extension to the multivariate case will be discussed a little later. During the observational study, the i.i.d. dataset $\bar{\mathcal{D}}_n = \{(X_i, Y_i, T_i) : 1 \leq i \leq n\}$ is collected with Y_i an abbreviation of $Y_i(T_i)$. Under the unconfoundedness assumption (2), our goal is to estimate the probability distribution $\pi_t(x, dy)$ associated with the conditional marginal distribution $\mathcal{L}(Y(t) \mid X = x)$ for $t \in \{0, 1\}$, based on the dataset $\bar{\mathcal{D}}_n$.

3.1   Wasserstein Random Forests for HTE

Before discussing the applications of these conditional marginal distribution estimations, we would like to stress again that we have no intention to "replace" the Average Treatment Effect-based causal inference strategy. On the contrary, our primary motivation is to provide a complementary tool so that a more transparent inference can be conducted, by maximizing the usage of available data. More precisely, we train WRF respectively on the treatment and control groups (3), to estimate respectively the conditional measures π_0 and π_1. These estimations are denoted by $\hat{\pi}_0$ and $\hat{\pi}_1$.

First, when potential outcomes are assumed to be univariate, a raw visualization of $\hat{\pi}_0$ and $\hat{\pi}_1$ is always accessible and informative. In this way, causality can therefore be visualized by the change of the shape of the marginal distributions. Next, following a philosophy similar to the CATE function, we propose to assess the changes in the conditional distribution in terms of Wasserstein distance using the criterion

$$\Lambda_p(x) = \mathcal{W}_p \left(\pi_0(x, dy), \pi_1(x, dy) \right).$$

Intuitively speaking, $\Lambda_p(\cdot)$ is capable of capturing certain causal effects that are less noticeable in terms of $\tau(\cdot)$. An estimation $\hat{\Lambda}_p(\cdot)$ can be obtained as a by-product of the estimation of $\hat{\pi}_0$ and $\hat{\pi}_1$. For practical implementation, a histogram of the estimation of $\Lambda_p(x)$ can be constructed by out-of-bag strategy. Finally, regarding the multivariate output case, we would like to mention that when the cost of the treatment, say

$C(1)$, is also collected in the dataset, WRF can then be used—as we have seen in Subsection 2.2, without further effort—to provide an estimation of the joint multivariate distribution $\mathcal{L}((Y(1), C(1)) \mid X = x)$ in order to conduct more complex inferences involving the costs and the treatment effects at the same time. The same idea also applies to the case where the treatment effects themselves are also multivariate.

3.2   Univariate conditional density estimation

Since the conditional distribution is in general inaccessible from the real-world datasets, we present here a simulation study based on synthetic data to illustrate the performance of WRF in the context of HTE, focusing on the conditional marginal distribution estimation. We consider the following model, where $X = (X^{(1)}, \ldots, X^{(d)})$ and the symbol $\mathcal{N}$ stands for the Gaussian distribution:

- $X \sim \mathrm{Unif}\left([0, 1]^d\right)$ with $d = 50$;
- $Y(0) \sim \mathcal{N}(m_0(X), \sigma_0^2(X))$;
- $Y(1) \sim \frac{1}{2}\delta_{-1} + \frac{1}{2}\mathcal{N}\left(m_1(X), \sigma_1^2(X)\right)$;
- $T \sim \mathrm{Bernoulli}\left(\frac{1}{2}\right)$;

with

- $m_0(x) = 10x^{(2)}x^{(4)} + x^{(3)} + \exp\left\{x^{(4)} - 2x^{(1)}\right\}$;
- $\sigma_0^2(x) = \left\{-x^{(1)}x^{(2)} + 4\left(x^{(3)}\right)^2\right\} \vee \frac{1}{5}$;
- $m_1(x) = 2m_0(x) + 1 - 5x^{(2)}x^{(5)}$;
- $\sigma_1^2(x) = 3x^{(2)} + x^{(3)}x^{(4)} + x^{(6)}$.

To summarize, the conditional measure $\pi_0(x, dy)$ is unimodal, while $\pi_1(x, dy)$ is bimodal, composed by a Gaussian and a Dirac at -1, and thus the conditional distribution of $Y(1)$ does not have a density w.r.t. Lebesgue measure. The mixture parameters $(1/2, 1/2)$ in π_1 can be interpreted as an unconfounding factor that is not collected in the study. The four functions $m_0(\cdot)$, $\sigma_0^2(\cdot)$, $m_1(\cdot)$, and $\sigma_1^2(\cdot)$ have been designed to implement complex dependence between the covariate and the potential outcomes. We note however that the CATE function takes the simple form $\tau(x) = -2.5x^{(2)}x^{(5)}$ and is therefore equal to zero if and only if $x^{(2)}x^{(5)} = 0$. The treatment and control groups are balanced due to the symmetrical form of T. This simple setting is usually referred to as *randomized study*. This choice allows us to avoid the complexity when dealing with the propensity score function, and we can thus focus on the conditional distribution estimation. A brief discussion on the influence of propensity score function can be found in **Supplementary Material**.

We trained the models based on a simulated dataset of size $n = 1000$, which is reasonably small considering the complexity of the conditional distribution estima-

---

Algorithm 2: Wasserstein Random Forests predicted distribution at $x \in \mathbb{R}^d$.

Require: Training dataset $\mathcal{D}_n$, number of trees $M > 0$, subsample size $a_n \in [n]$, Wasserstein order $p > 0$,
     mtry $\in [d]$ where d denotes the dimension of the covariate X, **nodesize** $\in [a_n]$ and $x \in \mathbb{R}^d$.

Result: The sequence of weights $(\alpha_i(x); i \in [n])$ which determines a weighted empirical measure that
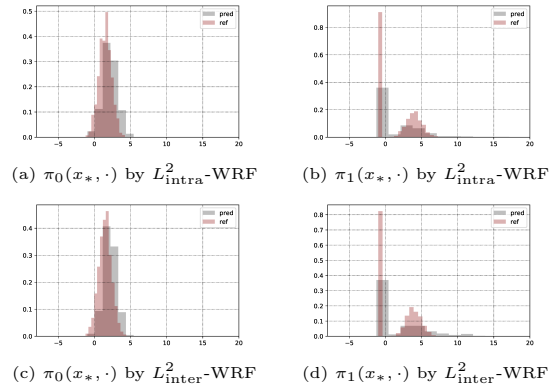   estimates the conditional distribution at x.

---

1 **for** $j \in \{1, 2, \ldots, M\}$ **do**

2   Select a_n points uniformly in $\mathcal{D}_n$, with or without replacement, as the sub-dataset $\mathcal{D}_n^*(\Theta_j)$.

3   Initiate a binary tree $\mathcal{T}(\Theta_j, \mathcal{D}_n)$ that only contains the root $\mathcal{D}_n^*(\Theta_j)$.

4   Set $\mathcal{P} = (\mathcal{D}_n^*(\Theta_j))$ the ordered list that contains the root of the tree.

5   **while** $\mathcal{P} \neq \varnothing$ **do**

6   Let A be the first element of $\mathcal{P}$.

7   **if** *A contains less data points than **nodesize** or if all $X_i \in A$ are identical* **then**

8   Remove the cell A from the list $\mathcal{P}$.

9   **else**

10   Select uniformly without replacement, a subset $\mathcal{M}_{try} \subset [d]$ of cardinality **mtry**.

11   Select the best split position z^* and the direction ℓ^* based on the sub-dataset A along the
             coordinates in $\mathcal{M}_{try}$ that maximizes the selected splitting rule (i.e., L^2_{intra} or L^p_{inter}). Cut A
             according to the best split. Denote respectively by A_L and A_R the corresponding cells.

12   Let the left and right children of A be respectively A_L and A_R, and associated the node A with
             the split position and direction (z^*, ℓ^*).

13   Remove the cell A from the list $\mathcal{P}$.

14   Concatenate $\mathcal{P}$, A_L and A_R.

15   **end**

16   **end**

17   Compute $\alpha_{i,j}(x) := \frac{\mathbf{1}_{\{X_i \in A_n(x;\Theta_j,\mathcal{D}_n)\}}}{M N_n(x;\Theta_j,\mathcal{D}_n)} \mathbf{1}_{N_n(x;\Theta_j,\mathcal{D}_n) > 0}$ for each $(X_i, Y_i) \in \mathcal{D}_n^*(\Theta_j)$ according to $\mathcal{T}(\Theta_j, \mathcal{D}_n)$.

18 **end**

19 Compute $\alpha_i(x) = \frac{1}{M} \sum_{j=1}^M \alpha_{i,j}(x)$ for each $i \in [n]$.

---

tion problem. An illustration for an individual x_* with $x_*^{(5)} = 0$ (so, $\tau(x_*) = 0$) can be found in Figure 2 ((a)-(b) for L^2_{intra}-WRF; (c)-(d) for L^2_{inter}-WRF). This visualization highlights the good quality of conditional inference performed by our WRF methods—both of them have highlighted the key properties such as multimodality and fluctuation in the conditional marginal distributions. More importantly, it stresses the pertinence of studying conditional distributions in the HTE context, since the CATE function, as is the case here, is not always capable to provide insights regarding causality. For example, according to the trained L^2_{intra}-WRF model, we have $\hat{\Lambda}_2(x_*) = 1.8591$ (reference value $\Lambda_2(x_*) = 2.1903$), which is much more noticeable as an indicator of causality than the CATE function (estimated by -0.3675) in this situation.

A finer comparison based on average Wasserstein distance is shown in Table 1 and Table 2, where π_t-$\overline{\mathcal{W}}_p(N)$ ($t = 0, 1$ and $p = 1, 2$) denotes the average $\mathcal{W}_p$-distance $1/2000 \sum_{i=1}^{2000} \mathcal{W}_p(\hat{\pi}_t(\tilde{X}_i, \cdot), \pi_t(\tilde{X}_i, \cdot))$, where $(\tilde{X}_i; 1 \leq i \leq 2000)$ are i.i.d. samples of $[0, 1]^d$-uniform random variables, which is basically a Monte-Carlo approximation of $\mathbb{E}\left[\mathcal{W}_p(\hat{\pi}_t(X, \cdot), \pi_t(X, \cdot)) \,\big|\, \bar{\mathcal{D}}_n\right]$. We compare several WRFs with other popular RF-based

(a) $\pi_0(x_*, \cdot)$ by L^2_{intra}-WRF   (b) $\pi_1(x_*, \cdot)$ by L^2_{intra}-WRF

(c) $\pi_0(x_*, \cdot)$ by L^2_{inter}-WRF   (d) $\pi_1(x_*, \cdot)$ by L^2_{inter}-WRF

Figure 2: An illustration of estimated conditional distributions provided by different variants of WRF with the same parameters: $a_n = 500$ (with repetition), $M = 200$, **mtry** $= 50$, **nodesize** $= 2$. In the legend, `pred` and `ref` denote respectively the histograms provided by WRF and reference values sampled directly from the true conditional distribution with sample sizes fixed to be 2000.

methods that are able to perform conditional distribution estimation. First, we consider Mondrian Forests (MF, Lakshminarayanan et al., 2014), whose splits do not depend on the response variable. The idea is to prove the relevance of our splitting criteria in the high-dimensional setting. Second, we consider Ex-

treme Randomized Trees (ERT, Geurts et al., 2006) with Breiman's rule. This can be seen as L^2_{intra}-WRF with different stochastic construction—the candidates of splitting positions are sampled uniformly on the edges of cells, and then the candidate with the best score w.r.t. L^2_{intra} is chosen. Finally, we also compare with another RF-based conditional distribution estimation method with different splitting rule (RFCDE, Pospisil and Lee, 2019) based on L^2-error of density estimations. We stress again that WRF do not need to assume that the conditional density w.r.t. lebesgue measure exists when dealing with conditional distribution estimation. Finally, we also compare with the classical Kernel Density Estimation (KDE, Rosenblatt, 1969) and its Nearest Neighbour counterpart (NN-KDE, Biau et al., 2015). We consider Gaussian kernel, with the smoothing bandwidth parameter h chosen by cross-validated grid-search (for the associated conditional expectation estimation), and the number of neighbours chosen to be the square root of the number of data points.

Table 1: Estimation of π_0 (i.e., $\mathcal{L}\left(Y(0) \mid X = x\right)$)

Methods	$\pi_0\text{-}\overline{\mathcal{W}}_1(1000)$	$\pi_0\text{-}\overline{\mathcal{W}}_2(1000)$
L^2_{intra}-WRF	0.7209	0.8809
L^2_{inter}-WRF	0.7150	0.8766
L^1_{inter}-WRF	**0.7097**	**0.8642**
MF	2.0835	2.4576
ERT	0.7736	0.9769
RFCDE	0.8111	0.9725
KDE	2.0110	2.5321
NN-KDE	1.9250	2.3961

Table 2: Estimation of π_1 (i.e., $\mathcal{L}\left(Y(1) \mid X = x\right)$)

Methods	$\pi_1\text{-}\overline{\mathcal{W}}_1(1000)$	$\pi_1\text{-}\overline{\mathcal{W}}_2(1000)$
L^2_{intra}-WRF	1.7030	2.8111
L^2_{inter}-WRF	1.3767	**2.2987**
L^1_{inter}-WRF	**1.3498**	2.3341
MF	2.2553	3.3778
ERT	1.6021	2.6742
RFCDE	3.2960	3.4895
KDE	2.3958	3.2993
NN-KDE	2.2490	3.1223

According to Table 1 and Table 2, it is clear that WRFs, especially L^1_{inter} version, provide promising results for this synthetic dataset. In particular, the good performance of L^p_{inter}-WRF w.r.t. L^2_{intra}-WRF may be connected to the discussion provided in Remark 2.3. Since the splits of MF do not depend on Y_i, it is easy to understand that most of splits are not performed at "good" directions. The method RFCDE is in general not easy to tune. Despite the choice of kernel,

we have used grid searching for determining the associated hyper parameters such as `bandwidth`. The poor performance in Table 2 may be explained by the non-existence of a probability density for π_1. It is interesting to note that ERT outperforms L^2_{intra}-WRF for the estimation of π_1, which suggests that there is still room to improve the stochastic construction of trees.

3.3 Multivariate case

We illustrate in this section the ability of L^2_{intra}-WRF when dealing with multivariate output. The implementation can be regarded as a natural generalization of Breiman's rule in the multivariate setting. Moreover, the complexity is optimal (linear) w.r.t. the dimension of Y. Denote by $C(1)$ the cost variable associated to the treatment, which is supposed to be a random variable that depends on X, namely, $C(1) \sim \mathcal{N}\left(2X^{(3)}X^{(5)} + X^{(2)}, X^{(5)}X^{(6)} + 1\right)$. Our goal is to estimate the joint conditional distribution $\mathcal{L}\left((Y(1), C(1)) \mid X = x\right)$. The basic setting of the algorithm remains the same as discussed in Section 3.2. As shown in Figure 3, L^2_{intra}-WRF gives, at least visually, a promising estimation of the conditional joint distribution even with only around 500 samples, which outperforms MF (Table 3). The results, again, provide evidence of the relevance of our Wasserstein distance-based interpretation in the multivariate case.
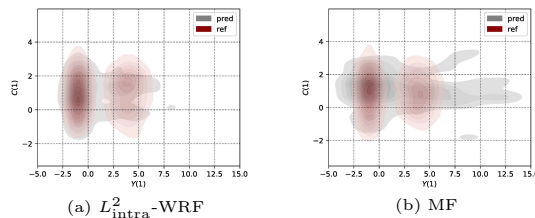
(a) L^2_{intra}-WRF (b) MF

Figure 3: An illustration of estimated conditional distributions (by heatmap) at a randomly selected point provided respectively by L^2_{intra}-WRF and MF.

Table 3: Estimation of $\mathcal{L}\left((Y(1), C(1)) \mid X = x\right)$

Methods	$\pi_1\text{-}\overline{\mathcal{W}}_1(1000)$	$\pi_1\text{-}\overline{\mathcal{W}}_2(1000)$
L^2_{intra}-WRF	0.0852	0.1298
MF	0.1055	0.1623

Conclusion

We have proposed a new approach based on WRF that can help HTE inference through estimating some key conditional distributions. From a theoretical perspective, the challenge is to prove consistency of WRF when the sample size tends to infinity, in the spirit of works such as Scornet et al. (2015); Wager (2014). For

example, a first goal would be to show that, under appropriate assumptions, $\mathbb{E}\left[\mathcal{W}_p(\hat{\pi}_t(X, \cdot), \pi_t(X, \cdot))\right] \to 0$ as $n \to \infty$, where $\hat{\pi}_t$ denotes the output of WRF and the expectation is taken w.r.t. both the distribution of X and the sample.

Acknowledgements

References

Athey, S., Tibshirani, J., and Wager, S. (2019). Generalized random forests. *The Annals of Statistics*, 47:1148–1178.

Athey, S. and Wager, S. (2019). Estimating treatment effects with causal forests: An application. *Observational Studies*, 5.

Biau, G., Cérou, F., and Guyader, A. (2015). New insights into approximate bayesian computation. *Annales de l'IHP Probabilités et statistiques*, 51(1):376–403.

Biau, G. and Scornet, E. (2015). A random forest guided tour. *TEST*, 25:197–227.

Breiman, L. (2001). Random forests. *Machine Learning*, 45:5–32.

Chernozhukov, V., Demirer, M., Duflo, E., and Fernández-Val, I. (2018). Generic machine learning inference on heterogeneous treatment effects in randomized experiments. Working Paper 24678, National Bureau of Economic Research.

Cuturi, M. (2013). Sinkhorn distances: Lightspeed computation of optimal transport. In Burges, C., Bottou, L., Welling, M., Ghahramani, Z., and Weinberger, K., editors, *Advances in Neural Information Processing Systems 26*, pages 2292–2300. Curran Associates, Inc.

Dutordoir, V., Salimbeni, H., Hensman, J., and Deisenroth, M. (2018). Gaussian process conditional density estimation. In Bengio, S., Wallach, H., Larochelle, H., Grauman, K., Cesa-Bianchi, N., and Garnett, R., editors, *Advances in Neural Information Processing Systems 31*, pages 2385–2395. Curran Associates, Inc.

Genevay, A., Chizat, L., Bach, F., Cuturi, M., and Peyré, G. (2019). Sample complexity of Sinkhorn divergences. In Chaudhuri, K. and Sugiyama, M., editors, *Proceedings of Machine Learning Research*, volume 89 of *Proceedings of Machine Learning Research*, pages 1574–1583. PMLR.

Geurts, P., Ernst, D., and Wehenkel, L. (2006). Extremely randomized trees. *Machine Learning*, 63:3–42.

Hall, P., Wolff, R. C., and Yao, Q. (1999). Methods for estimating a conditional distribution function. *Journal of the American Statistical Association*, 94:154–163.

Hall, P. and Yao, Q. (2005). Approximating conditional distribution functions using dimension reduction. *The Annals of Statistics*, 33:1404–1421.

Hothorn, T. and Zeileis, A. (2017). Transformation forests. *arXiv preprint arXiv:1701.02110*.

Imbens, G. W. and Rubin, D. B. (2015). *Causal Inference for Statistics, Social, and Biomedical Sciences: An Introduction*. Cambridge University Press, Cambridge.

Künzel, S. R., Sekhon, J. S., Bickel, P. J., and Yu, B. (2019). Metalearners for estimating heterogeneous treatment effects using machine learning. *Proceedings of the National Academy of Sciences*, 116:4156–4165.

Lakshminarayanan, B., Roy, D. M., and Teh, Y. W. (2014). Mondrian forests: Efficient online random forests. In Ghahramani, Z., Welling, M., Cortes, C., Lawrence, N. D., and Weinberger, K. Q., editors, *Advances in Neural Information Processing Systems 27*, pages 3140–3148. Curran Associates, Inc.

Lin, T., Ho, N., and Jordan, M. I. (2019). On the efficiency of the Sinkhorn and Greenkhorn algorithms and their acceleration for optimal transport. *arXiv*, 1906.01437.

Meinshausen, N. (2006). Quantile regression forests. *Journal of Machine Learning Research*, 7:983–999.

Miller, K., Huettmann, F., Norcross, B., and Lorenz, M. (2014). Multivariate random forest models of estuarine-associated fish and invertebrate communities. *Marine Ecology Progress Series*, 500:159–174.

Nie, X. and Wager, S. (2017). Quasi-oracle estimation of heterogeneous treatment effects. *arXiv*, 1712.04912.

Peyré, G. and Cuturi, M. (2018). Computational Optimal Transport. *arXiv*, 1803.00567.

Pospisil, T. and Lee, A. B. (2019). RFCDE: Random Forests for Conditional Density Estimation and functional data. *arXiv*, 1906.07177.

Rosenblatt, M. (1969). Conditional probability density and regression estimators. *Multivariate analysis II*, 25:31.

Rubin, D. (1974). Estimating causal effects of treatments in randomized and nonrandomized studies. *Journal of Educational Psychology*, 66:688–701.

Santambrogio, F. (2015). *Optimal transport for applied mathematicians*, volume 55. Springer.

Scornet, E., Biau, G., and Vert, J.-P. (2015). Consistency of random forests. *The Annals of Statistics*, 43:1716–1741.

Segal, M. and Xiao, Y. (2011). Multivariate random forests. *WIREs Data Mining and Knowledge Discovery*, 1:80–87.

Wager, S. (2014). Asymptotic theory for random forests. *arXiv*, 1405.0352.